Journal of Biomolecular NMR, **19:** 331–345, 2001.
KLUWER/ESCOM

$^{13}C_\alpha$ and $^{13}C_\beta$ chemical shifts as a tool to delineate β-hairpin structures in peptides

Clara M. Santiveri, Manuel Rico & M. Angeles Jiménez*
Instituto de Estructura de la Materia, Consejo Superior de Investigaciones Científicas, Serrano 119, E-28006 Madrid, Spain

Received 7 November 2000; Accepted 18 January 2001

Key words: ^{13}C chemical shifts, β-hairpin, β-hairpin quantification, peptide structure, β-turn

Abstract

Unravelling the factors that contribute to the formation and the stability of β-sheet structure in peptides is a subject of great current interest. A β-hairpin, the smallest β-sheet motif, consists of two antiparallel hydrogen-bonded β-strands linked by a loop region. We have performed a statistical analysis on protein β-hairpins showing that the most abundant types of β-hairpins, 2:2, 3:5 and 4:4, have characteristic patterns of $^{13}C_\alpha$ and $^{13}C_\beta$ conformational shifts, as expected on the basis of their φ and ψ angles. This fact strongly supports the potential value of $^{13}C_\alpha$ and $^{13}C_\beta$ conformational shifts as a means to identify β-hairpin motifs in peptides. Their usefulness was confirmed by analysing the patterns of $^{13}C_\alpha$ and $^{13}C_\beta$ conformational shifts in 13 short peptides, 10–15 residues long, that adopt β-hairpin structures in aqueous solution. Furthermore, we have investigated their potential as a method to quantify β-hairpin populations in peptides.

Abbreviations: 1D, 2D, one-, two-dimensional; Δδ, conformational shift; COSY, homonuclear correlated spectroscopy; HSQC, heteronuclear single quantum coherence spectroscopy; NOE, nuclear Overhauser effect; NOESY, nuclear Overhauser enhancement spectroscopy; ppm, parts per million; ROESY, rotating frame NOE spectroscopy; TOCSY, total correlation spectroscopy; TSP, sodium [3-trimethylsilyl 2,2,3,3-$^2H_4$] propionate.

Introduction

The interpretation of NMR parameters in terms of structure in peptides is not straightforward because, in contrast to proteins, linear peptides do not adopt a single structure, but they exist as ensembles of transient interconverting structures in fast exchange on the NMR time scale (Wright et al., 1988; Dyson and Wright, 1991; Daura et al., 1999). The observed NMR parameters, chemical shifts and coupling constants are averaged values over all existing conformations, and NOE connectivities can be detected for all significantly populated conformations. Even using a simplified analysis which considers only two sets of structures, one set corresponding to folded conformations and the other to the random coil state, it is not trivial to confirm the existence of a folded structure, its nature and its weight within the ensemble. Since different NMR parameters are differently affected by peptide conformation, it would be advisable in solving the problem to use as many available parameters as possible. ^{13}C chemical shifts have hardly been used in peptide conformational studies so far, and we think that adding the structural information derived from them to that obtained from other NMR parameters would contribute to a better structural analysis of peptides.

$^{13}C_\alpha$ and $^{13}C_\beta$ chemical shifts have recently found application in refining protein NMR structures (Laws et al., 1993; Kuszewski et al., 1995; Le et al., 1995; Luginbühl et al., 1995; Oldfield, 1995; Beger and Bolton, 1997; Cornilescu et al., 1999) once their relationships to φ and ψ backbone dihedral angles have been established. Regular elements of secondary

*To whom correspondence should be addressed. E-mail: angeles@malika.iem.csic.es

DISK Gr.: 201022619, JNMR K0067R (jnmrkap:bio2fam) v.1.1
jn333537.tex; 28/03/2001; 11:06; p.1

structure, helices and strands, show characteristic $^{13}C_\alpha$ and $^{13}C_\beta$ conformational shifts (Spera and Bax, 1991; de Dios et al., 1993; Wishart and Sykes, 1994; Szilágyi, 1995; Iwadate et al., 1999). Conformational shifts are defined as the deviations of the $^{13}C_\alpha$ and $^{13}C_\beta$ chemical shifts relative to their corresponding random coil values ($\Delta\delta_{^{13}C} = \delta_{observed} - \delta_{random\ coil}$, ppm). In particular, $^{13}C_\alpha$ conformational shifts have been recognised as a useful and sensitive parameter to detect and identify secondary structure (Buckley et al., 1993; Gronenborn and Clore, 1994; Yao et al., 1997; Guerois et al., 1998). Unlike $C_\alpha H$ chemical shifts, which are broadly used in delineating secondary structural elements of proteins and in conformational studies of peptides (Case et al., 1994; Ösapay and Case, 1994; Wishart and Sykes, 1994; Szilágyi, 1995) in spite of being normally affected by aromatic ring current effects, $^{13}C_\alpha$ and $^{13}C_\beta$ chemical shifts are mainly determined by the ϕ and ψ backbone dihedral angles (Spera and Bax, 1991; de Dios et al., 1993; Wishart and Sykes, 1994; Iwadate et al., 1999). This suggests that the patterns of $^{13}C_\alpha$ and $^{13}C_\beta$ conformational shifts could in principle be used to identify not only regular elements of secondary structure but also different structural motifs in peptides. For example, a pattern that can be used as an indicator of an N-terminal capping box, whose N-cap residue has characteristic ϕ and ψ angles, has been found by analysis of $^{13}C_\alpha$ and $^{13}C_\beta$ chemical shifts in a set of 11 proteins (Gronenborn and Clore, 1994). The $^{13}C_\alpha$ conformational shifts have also been used in conjunction with other NMR parameters in a few structural studies on peptides adopting α-helices (Lee et al., 1992; Reily et al., 1992; Buckley et al., 1993; Guerois et al., 1998) and β-sheet motifs (de Alba et al., 1999a; Santiveri et al., 2000).

Currently great interest exists in unravelling the factors contributing to the formation and stability of β-sheet motifs in isolated peptides (Smith and Regan, 1997; Blanco et al., 1998; Gellman, 1998; Lacroix et al., 1999; Ramírez-Alvarado et al., 1999). A β-hairpin, the simplest β-sheet motif, consists of two antiparallel hydrogen-bonded β-strands linked by a loop region. β-Hairpin motifs differ in the length and shape of the loop region and are classified according to the number of residues in the turn and the number of interstrand hydrogen bonds between residues flanking the turn (Figure 1; Sibanda and Thornton, 1985, 1991; Sibanda et al., 1989). It is well known that in the strands of β-hairpin motifs the $^{13}C_\alpha$ conformational shifts are negative and the $^{13}C_\beta$ conformational shifts positive. The pattern of $^{13}C_\alpha$ and $^{13}C_\beta$ conformational shifts in the connecting region will depend on their conformation. Thus, once having obtained known relationships between $^{13}C_\alpha$ and $^{13}C_\beta$ chemical shifts and ϕ and ψ dihedral angles, one should expect a pattern of $^{13}C_\alpha$ and $^{13}C_\beta$ conformational shifts characteristic of each type of β-hairpin.

This idea prompted us to investigate the applicability of $^{13}C_\alpha$ and $^{13}C_\beta$ conformational shift patterns in delineating β-hairpin motifs in peptides. First, we compared the patterns of $^{13}C_\alpha$ and $^{13}C_\beta$ conformational shifts expected for the different types of β-hairpins with those found in proteins. Second, we tested their applicability to identify β-hairpin motifs in peptides by analysing the profiles of $^{13}C_\alpha$ and $^{13}C_\beta$ conformational shifts exhibited by several available examples of peptides that adopt β-hairpin structures in aqueous solution. Finally, we investigated their potential as a method to quantify β-hairpin populations in peptides. To this end, we analysed the correlation between the β-hairpin populations estimated from the average of the $^{13}C_\alpha$ and $^{13}C_\beta$ conformational shifts within the β-strands and those obtained from the intensity of $C_\alpha H_k$-$C_\alpha H_j$ NOEs, where k and j are facing residues in a non-hydrogen-bonded site (Figure 1), as well as those resulting from the averaged β-strand $C_\alpha H$ conformational shifts.

Materials and methods

Peptide synthesis and purification

Peptides h2 and h11 were chemically synthesised by DiverDrugs (Barcelona, Spain) and peptide h10 by the Peptide Synthesis Facility at the Department of Organic Chemistry (University of Barcelona, Spain). The synthesis and purification of the other 10 peptides was previously reported (see references in Table 1).

NMR spectra

Peptide samples for NMR experiments were prepared in 0.5 ml of H_2O/D_2O (9:1 ratio by volume) or in D_2O. Peptide concentrations were about 1–5 mM. pH was measured with a glass micro electrode and was not corrected for isotope effects. The temperature of the NMR probe was calibrated using a methanol sample. Sodium [3-trimethylsilyl 2,2,3,3-$^2H_4$] propionate (TSP) was used as an internal reference. The ^{1}H-NMR spectra were acquired on a Bruker AMX-600 pulse spectrometer operating at a proton frequency of 600.13 MHz. 1D spectra were acquired

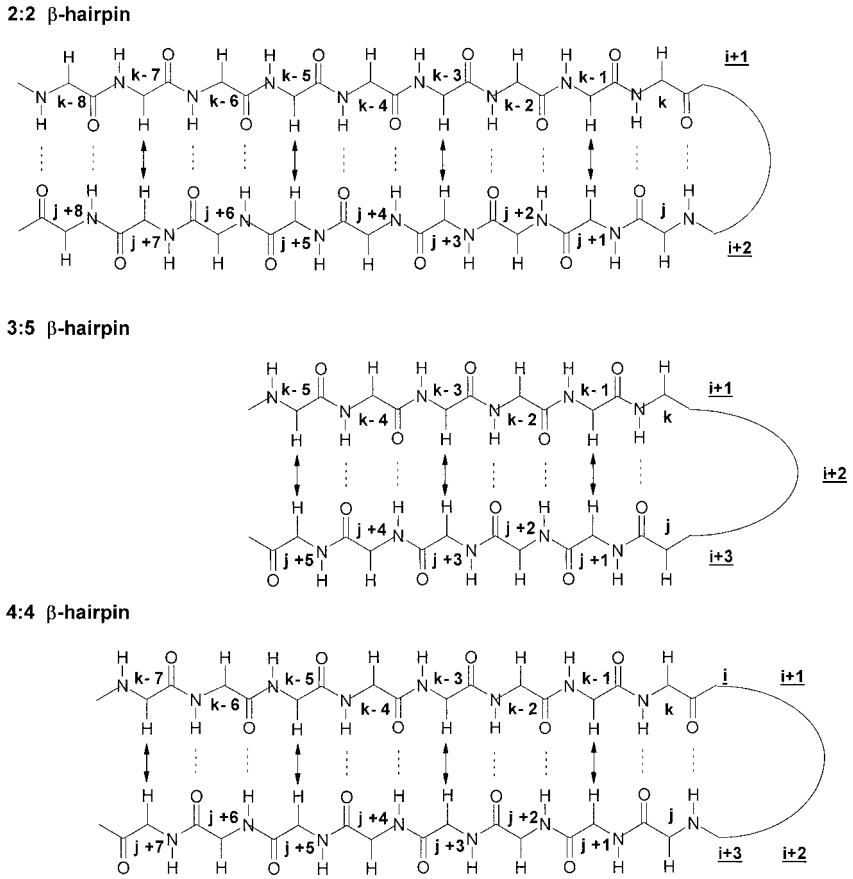

Figure 1. Backbone schematic representation of the strands in 2:2, 3:5, and 4:4 β-hairpins and nomenclature of residues (in bold). Turn residues are underlined. Dotted lines indicate hydrogen bonds, and black arrows connect the $C_\alpha H$ protons that give rise to NOEs. A pair of facing residues is in a non-hydrogen-bonded site when their CO and NH are not hydrogen-bonded.

using 32K data points, which were zero-filled to 64K data points before performing the Fourier transformation. Phase-sensitive two-dimensional correlated spectroscopy (COSY; Aue et al., 1976), total correlated spectroscopy (TOCSY; Rance, 1987), nuclear Overhauser enhancement spectroscopy (NOESY; Jeener et al., 1979; Kumar et al., 1980) and rotating frame nuclear Overhauser effect spectroscopy (ROESY; Bothner-By et al., 1984; Braunschweiler and Ernst, 1983) spectra were recorded by standard techniques using presaturation of the water signal and the time-proportional phase incrementation mode (Redfield and Kuntz, 1975). NOESY and ROESY mixing times were 200 ms and 120 ms, respectively. TOCSY spectra were recorded using 80 ms MLEV17 with a z filter spin-lock sequence (Rance, 1987). The ^{1}H-^{13}C heteronuclear single quantum coherence spectroscopy (HSQC; Bodenhausen and Ruben, 1980) spectra at natural ^{13}C abundance were recorded in D_2O samples. Acquisition data matrices were defined by 2048 $\times$ 512 points in t_2 and t_1, respectively. Data were processed using the standard XWIN-NMR Bruker program on a Silicon Graphics computer. The 2D data matrix was multiplied by a square-sine-bell window function with the corresponding shift optimised for every spectrum and zero-filled to a 2K $\times$ 1K complex matrix prior to Fourier transformation. Baseline correction was applied to both dimensions. The 0 ppm ^{13}C δ was obtained indirectly by multiplying the spectrometer frequency that corresponds to 0 ppm in the ^{1}H spectrum, assigned to an internal TSP reference, by 0.25144954 (Bax and Subramanian, 1986; Spera and Bax, 1991).

NMR assignment

The ^{1}H NMR signals of peptides h1, h2, h10, h11 and h13 in aqueous solution were readily assigned by standard sequential assignment methods (Wüthrich

Table 1. List of analysed peptides and β-hairpin populations estimated by quantification methods based on different NMR parameters, as described in the text. The β-strand residues are underlined. The numbers of residues used to calculate the populations from Δδ values are given in parentheses. The $\Delta\delta_{^{13}C\alpha}$- and $\Delta\delta_{^{13}C\beta}$-based populations estimated by using as reference for the 100% β-hairpin the values reported by Spera and Bax (1991) and those from this paper are shown in standard and in bold font styles, respectively. The populations obtained by excluding the anomalous $\Delta\delta_{^{13}C\alpha}$, $\Delta\delta_{^{13}C\beta}$ and $\Delta\delta_{C\alpha H}$ values (those with sign opposite to that characteristic of a strand residue or with a null value) are given in italics. The averaged β-hairpin population showing the lowest standard deviation is underlined

Peptide	Sequence	β-Hairpin type[a]	β-Hairpin percentage estimated from				
			NOE	$\Delta\delta_{C\alpha H}$[b]	$\Delta\delta_{^{13}C\alpha}$[b]	$\Delta\delta_{^{13}C\beta}$[b]	Average[c]
h1	K1 T W T N	2:2 I′	20	12±3 (6)	20±7 (6)	11±5 (6)	16±5
					19±6 (6)	**14±6 (6)**	**16±4**
	T10 S I K G				*19±3 (4)*	*20±7 (6)*	*13±5 (5)*	*18±3*
					19±6 (6)	***16±6 (5)***	***19±2***
h2	S1 E S Y I Y N	2:2 I′	40	19±3 (10)	24±7 (10)	22±5 (10)	26±9
					23±6 (10)	**28±6 (10)**	**28±9**
	E14 T V T W K G				*29±3 (8)*	*29±7 (9)*	*28±5 (8)*	*31±6*
					27±6 (9)	***37±6 (8)***	***33±6***
h3	T1 W I Q N G	2:2 II′	16	0±3 (8)	15±7 (8)	5±5 (8)	9±8
					14±6 (8)	**6±6 (8)**	**9±7**
	Q12 Y W K T S				*13±3 (2)*	*33±7 (4)*	*8±5 (5)*	*17±11*
					31±6 (4)	***11± 6 (5)***	***18±9***
h4	K1 W Y Q N G	2:2 II′	17	0±3 (8)	16±7 (8)	18±5 (8)	13±9
					15±6 (8)	**23±6 (8)**	**14±10**
	T12 Y I K T S				*28±3 (2)*	*20±7 (7)*	*18±5 (8)*	*21±5*
					19±6 (7)	***23±6 (8)***	***21±5***
h5	S1 Y I N S	3:5 I+G1	47	24±3 (5)	43±7 (5)	26±5 (5)	35±12
	D	β-bulge			**40±6 (5)**	**34±6 (5)**	**36±10**
	T10 W T G				*45±3 (4)*	*43±7 (5)*	*36±5 (4)*	*43±5*
					40±6 (5)	***47±6 (4)***	***45±3***
h6	Y1 I T N S	3:5 I+G1	76	44±3 (5)	27±7 (5)	25±5 (5)	43±24
	D	β-bulge			**25±6 (5)**	**33±6 (5)**	**45±22**
	T10 W T G				*58±3 (4)*	*44±7 (3)*	*35±5 (4)*	*53±18*
					42±6 (3)	***46±6 (4)***	***56±15***
h7	T1 I S N S	3:5 I+G1	13	9±3 (5)	11±7 (5)	5±5 (5)	9±3
	D	β-bulge			**9±6 (5)**	**7±6 (5)**	**9±3**
	T10 W T G				*20±3 (3)*	*18±7 (3)*	*12±5 (3)*	*16±4*
					17±6 (3)	***16±6 (3)***	***17±3***
h8	S1 E I Y S N P	3:5 I+G1	47	44±3 (10)	43±7 (10)	29±5 (10)	41±8
	D	β-bulge			**40±6 (10)**	**38±6 (10)**	**45±7**
	E15 T V T W T G				*54±3 (9)*	*43±7 (10)*	*39±5 (8)*	*46±6*
					40±6 (10)	***51±6 (8)***	***48±6***
h9	S1 E S Y I N S	3:5 I+G1	63	46±3 (10)	41±7 (10)	38±5 (9)	46±12
	D	β-bulge			**38±6 (10)**	**49±6 (9)**	**49±11**
	E15 T V T W T G				*62±3 (9)*	*44±7 (9)*	*38±5 (9)*	*52±13*
					41±6 (9)	***49±6 (9)***	***54±11***
h10	S1 E S Y I N P	3:5 I+G1	60	55±3 (10)	41±7 (10)	29±5 (10)	48±12
	D	β-bulge			**38±6 (10)**	**38±6 (10)**	**49±10**
	E15 T V T W T G				*73±3 (9)*	*49±7 (9)*	*45±5 (8)*	*57±12*
					46±6 (9)	***58±6 (8)***	***59±11***

Table 1 (continued)

Peptide	Sequence	β-Hairpin type[a]	β-Hairpin percentage estimated from				
			NOE	$\Delta\delta_{C\alpha H}$[b]	$\Delta\delta_{^{13}C\alpha}$[b]	$\Delta\delta_{^{13}C\beta}$[b]	Average[c]
h11	S1 E S Y I N S	3:5 I+G1	48	50±3 (10)	28±7 (10)	31±5 (10)	39±11
	D	β-bulge			**26±6 (10)**	**41±6 (10)**	**41±11**
	E15 T V T V T G			*50±3 (10)*	*38±7 (8)*	*36±5 (9)*	*43±7*
					36±6 (8)	***47±6 (9)***	***45±6***
h12	I1 Y S A K	4:4 I	31	0±3 (4)	35±7 (4)	2±5 (4)	17±19
					33±6 (4)	**3±6 (4)**	**17±18**
	T10 W T G A			*24±3 (2)*	*56±7 (3)*	*9±5 (2)*	*30±20*
					52±6 (3)	***12±6 (2)***	***30±17***
h13	S1 Y I A K	4:4 I	5	0±3 (4)	28±7 (4)	3±5 (4)	9±13
					27±6 (4)	**4±6 (4)**	**9±12**
	T10 W T G A			*21±3 (2)*	*40±7 (3)*	*7±5 (2)*	*18±16*
					38±6 (3)	***9±6 (2)***	***18±15***

[a]As determined from NMR parameters, mainly the set of non-sequential NOEs. The corresponding references are: de Alba (1997) for peptides h1 and h13; de Alba et al. (1999a) for peptides h3 and h4; de Alba et al. (1997a) for peptides h5, h6 and h7; de Alba et al. (1999b) for peptide h8; Santiveri et al. (2000) for peptide h9; de Alba et al. (1997b) for peptide h12. A detailed NMR conformational study for peptides h2, h10 and h11 will be reported elsewhere (Santiveri, Rico and Jiménez, in preparation).
[b]To calculate the reported errors, the experimental errors in measuring the ^{1}H and ^{13}C δ values were assumed to be equal to ±0.01 ppm and ±0.1 ppm, respectively.
[c]The reported errors correspond to the standard deviation.

Table 2. R-values and slopes for the correlation between the β-hairpin population formed by the peptides listed in Table 1 as estimated from different NMR parameters, NOE intensity, $\Delta\delta_{C\alpha H}$, $\Delta\delta_{C\alpha}$ and $\Delta\delta_{C\beta}$, as described in the text, and the populations averaged for the four methods

		Averaged β-hairpin population			
		All strand values[a]		Excluding anomalous values[b]	
		Bax[c]	This paper[d]	Bax[c]	This paper[d]
NOE	r	0.95	0.94	0.96	0.96
	slope	1.37±0.06	1.31±0.06	1.13±0.06	1.09±0.05
$\Delta\delta_{C\alpha H}$	r	0.96	0.96	0.97	0.97
	slope	0.98±0.09	0.97±0.08	1.13±0.04	1.09±0.04
$\Delta\delta_{C\alpha}$	r	0.74	0.73	0.67	0.66
	slope	0.93±0.09	0.83±0.09	0.99±0.09	0.89±0.08
$\Delta\delta_{C\beta}$	r	0.93	0.94	0.93	0.94
	slope	0.72±0.04	0.90±0.05	0.75±0.04	0.94±0.05

[a]The $\Delta\delta_{C\alpha H}$, $\Delta\delta_{C\alpha}$ and $\Delta\delta_{C\beta}$ values measured for all the strand residues are considered to estimate the β-hairpin population.
[b]The $\Delta\delta_{C\alpha}$, $\Delta\delta_{C\beta}$ and $\Delta\delta_{C\alpha H}$ with sign opposite to that corresponding to a strand residue or with a null value are not included in the estimation of the β-hairpin population.
[c]The averaged $\Delta\delta_{C\alpha}$ and $\Delta\delta_{C\beta}$ values in protein sheets reported by Spera and Bax (1991) are taken as reference for the 100% β-hairpin.
[d]The averaged $\Delta\delta_{C\alpha}$ and $\Delta\delta_{C\beta}$ values obtained for strand residues in β-hairpins obtained here are used for the 100% β-hairpin reference.

et al., 1984; Wüthrich, 1986). The ^{1}H assignments of peptides h5, h6, h7, h8 and h12 were taken from the references in Table 1. Then, the ^{13}C resonances were straightforwardly assigned on the basis of the cross-correlations observed in the HSQC spectra between the proton and the carbon to which it is bonded. The ^{1}H and ^{13}C δ-values of peptides h3, h4 and h9 were previously reported (references in Table 1). The ^{1}H and ^{13}C δ-values of peptides h1, h2, h5, h6, h7, h8, h10, h11, h12 and h13 are available as Supplementary material (Tables SM3–SM12) and have been deposited in the PESCADOR database (http://ucmb.ulb.ac.be/Pescador/).

Estimation of β*-hairpin populations*

The β-hairpin populations for all peptides were estimated from the ratio of intensities of the $C_\alpha H_k$-$C_\alpha H_j$ NOE characteristic of each hairpin to that of the conformationally independent C_αH-$C_{\alpha'}$H Gly NOE, which was used for calibration purposes (Searle et al., 1995; de Alba et al., 1996, 1997a, b; Ramírez-Alvarado et al., 1996; Maynard et al., 1998). The intensity ratio corresponding to a 100% β-hairpin was taken as $[d_{C\alpha H_k - C\alpha H_j}]^{-6}$ / $[d_{C\alpha H - C\alpha' H\ Gly}]^{-6}$, where $d_{C\alpha H_k - C\alpha H_j}$ is the average $C_\alpha H_k$-$C_\alpha H_j$ distance in antiparallel β-sheets in proteins (2.3 Å; Wüthrich, 1986), where k and j are facing residues in a non-hydrogen-bonded site, and $d_{C\alpha H - C\alpha' H\ Gly}$ is the C_αH-$C_{\alpha'}$H distance characteristic of Gly residues (1.78 Å). NOE intensities were measured by volume integration in NOESY spectra (200 ms mixing time) recorded in D_2O samples.

The β-hairpin populations were independently evaluated by using the $\Delta\delta_{C\alpha H}$ ($\delta_{C\alpha H(observed)} - \delta_{C\alpha H(random\ coil)}$), $\Delta\delta_{^{13}C\alpha}$ ($\delta_{^{13}C\alpha(observed)} - \delta_{^{13}C\alpha(random\ coil)}$) and $\Delta\delta_{^{13}C\beta}$ ($\delta_{^{13}C\beta(observed)} - \delta_{^{13}C\beta(random\ coil)}$) conformational shifts averaged over all the strand residues in the adopted hairpins, except for the N- and C-terminal residues that have charge end effects. The reference values for each residue in the random coil state were taken from Bundi and Wüthrich (1979) for proton chemical shifts ($\delta_{C\alpha H(random\ coil)}$) and from Wishart et al. (1995a) for carbon chemical shifts ($\delta_{^{13}C\alpha(random\ coil)}$ and $\delta_{^{13}C\beta(random\ coil)}$). Since these ^{13}C δ-values are referenced to DSS and peptides h1–h13 to TSP, the corresponding correction was applied (≈ 0.1 ppm; Wishart et al., 1995b). The reference values for 100% β-hairpin were the mean conformational shifts reported for β-sheet proteins, 0.40 ppm for $\Delta\delta_{C\alpha H}$ (Wishart et al., 1991), −1.5 ppm (Spera and Bax, 1991) or −1.6 (this paper) for $\Delta\delta_{^{13}C\alpha}$, and 2.2 ppm (Spera and Bax, 1991) or 1.7 (this paper) for $\Delta\delta_{^{13}C\beta}$.

Protein ^{13}*C chemical shift database analysis*

A protein database including the ^{13}C chemical shifts of 40 proteins (Iwadate et al., 1999) has been used. From this database, we selected those proteins whose structures contain at least one β-hairpin motif (Supplementary Table SM1) according to the results from Promotif analysis provided at PDBsum (http://www.biochem.ucl.ac.uk/bsm/pdbsum/index.html).

Results

Analysis of $^{13}C_\alpha$ *and* $^{13}C_\beta$ *chemical shifts in protein* β*-hairpins*

To get the averaged profiles of the $^{13}C_\alpha$ and $^{13}C_\beta$ conformational shifts of the different types of β-hairpins, we have performed a statistical analysis on protein β-hairpins with available ^{13}C δ assignments. We then selected the 23 proteins that contain β-hairpin motifs in their structure from the set of 40 proteins used by Iwadate et al. (1999) in their recent study of the factors affecting ^{13}C chemical shifts. We restricted the survey to the most abundant types of β-hairpins, i.e., 2:2, 3:5 and 4:4 β-hairpins (Sibanda and Thornton, 1985, 1991; Sibanda et al., 1989), which contain short loops, since loops longer than 4 residues in β-hairpins do not show a common conformation. In total, we have examined 21 2:2 β-hairpins, 11 with a type I′ β-turn and 10 with a type II′ β-turn, 8 3:5 β-hairpins and 3 4:4 β-hairpins (cf Supplementary material, Table SM1). The longest 2:2 and 4:4 β-hairpins have 20 residues while the longest 3:5 β-hairpins contain only 15 residues. The $\Delta\delta_{^{13}C\alpha}$ and $\Delta\delta_{^{13}C\beta}$ values were obtained for each position by using the set of random coil values reported by Wishart et al. (1995a). The nomenclature used for the residues at each position is given in Figure 1. The 2:2 β-hairpins with types I′ and II′ β-turns were analysed separately. The resulting averaged $\Delta\delta_{^{13}C\alpha}$ and $\Delta\delta_{^{13}C\beta}$ profiles are shown in Figure 2.

As expected, the strand residues show negative $\Delta\delta_{^{13}C\alpha}$ and positive $\Delta\delta_{^{13}C\beta}$ values (Figure 2). The averaged $\Delta\delta_{^{13}C\alpha}$ and $\Delta\delta_{^{13}C\beta}$ values for strand residues in the analysed β-hairpins are -1.6 ± 1.3 ppm (mean of 313 values) and $+1.7 \pm 1.8$ ppm (mean of 240 values), respectively, where the reported errors are the standard deviations. These values are in agreement with

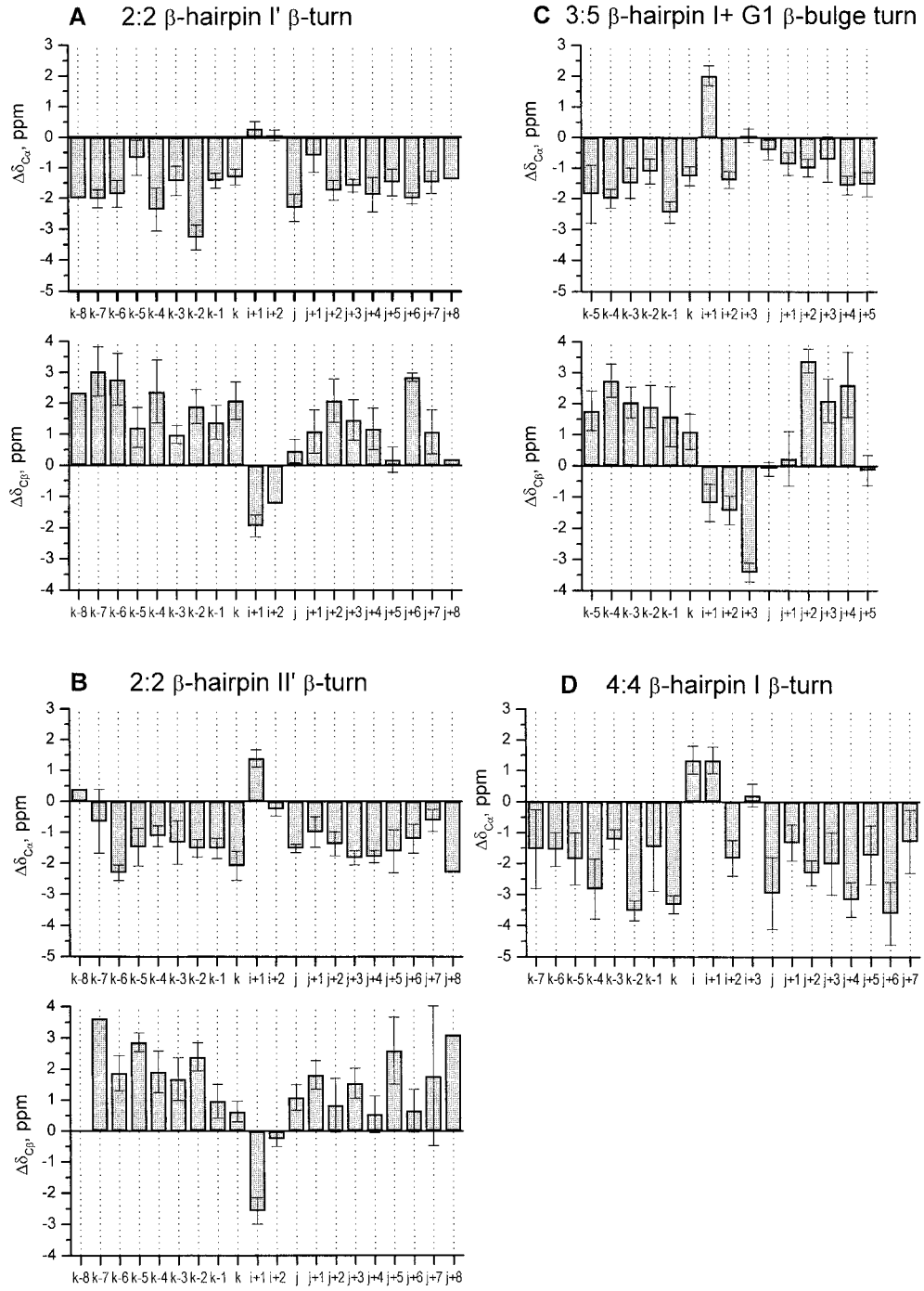

Figure 2. Averaged $^{13}C_{\alpha}$ and $^{13}C_{\beta}$ conformational shifts ($\Delta\delta = \delta_{(obs)} - \delta_{(random\ coil)}$ (ppm) where $\delta_{^{13}C\alpha(random\ coil)}$ and $\delta_{^{13}C\beta(random\ coil)}$ values were taken from Wishart et al. (1995a)) as a function of residue position, named according to the nomenclature in Figure 1, for the most abundant protein β-hairpins. (A) 2:2 β-hairpins with a type I′ β-turn, (B) 2:2 β-hairpins with a type II′ β-turn, (C) 3:5 β-hairpins with a type I + G1 β-bulge turn, and (D) 4:4 β-hairpins with a type I β-turn. Error bars correspond to standard errors at each position.

those previously reported by considering 126 β-sheet residues, -1.5 ± 1.2 and $+2.2 \pm 1.9$ ppm for $\Delta\delta_{^{13}C\alpha}$ and $\Delta\delta_{^{13}C\beta}$, respectively (Spera and Bax, 1991). The large standard deviations are probably caused by the large variation in the ϕ and ψ angles of the analysed strand residues, $-116 \pm 31°$ and $134 \pm 29°$, respectively. It has been previously observed that ϕ and ψ angles show a broader distribution in strand residues than in helix residues (Spera and Bax, 1991). In a minority of the strand residues, the $\Delta\delta_{^{13}C\alpha}$ and/or $\Delta\delta_{^{13}C\beta}$ values have the opposite sign to the one expected. This occurs more frequently for C_β carbons (17%) than for C_α carbons (8%). The effect of backbone conformation is likely to be stronger for C_α carbons than for C_β carbons. In many of these residues, the ϕ angle lies outside the characteristic β-sheet range, $|\phi| < 90°$ in most cases. This angle variation translates into a less negative $\Delta\delta_{^{13}C\alpha}$ value and even a sign change of the $\Delta\delta_{^{13}C\beta}$ value according to the relationship between ϕ and ψ angles and the $^{13}C_\alpha$ and $^{13}C_\beta$ conformational shifts (Iwadate et al., 1999). The fact that the pH dependence of the chemical shifts is not taken into account in the reference data (Wishart et al., 1995a) can explain why some charged residues have $\Delta\delta_{^{13}C\alpha}$ and/or $\Delta\delta_{^{13}C\beta}$ values lying outside the expected range.

The patterns of $^{13}C_\alpha$ and $^{13}C_\beta$ conformational shifts found for the four analysed types of β-hairpin motifs differ at the turn region, but all of them have at least one residue with a positive $\Delta\delta_{^{13}C\alpha}$ value and a negative $\Delta\delta_{^{13}C\beta}$ value (Figure 2). There are no $^{13}C_\beta$ chemical shift data available for 4:4 β-hairpins. The $\Delta\delta_{^{13}C\alpha}$ and $\Delta\delta_{^{13}C\beta}$ ranges expected for each position of the turn region in the different β-hairpin types (Figure 3) were obtained by analysis of the maps of $\Delta\delta_{^{13}C\alpha}$ and $\Delta\delta_{^{13}C\beta}$ shielding surfaces as a function of ϕ and ψ angles (Spera and Bax, 1991; Iwadate et al., 1999). The ϕ and ψ angles of each residue were taken from its location on the Ramachandran map (Sibanda et al., 1989; Sibanda and Thornton, 1991). The $\Delta\delta_{^{13}C\alpha}$ and $\Delta\delta_{^{13}C\beta}$ patterns observed for the four β-hairpin motifs in proteins coincide with those expected on the basis of their characteristic ϕ and ψ angles (see Figures 2 and 3).

Profiles of $^{13}C_\alpha$ and $^{13}C_\beta$ conformational shifts found in β-hairpin forming peptides

Since the different β-hairpin motifs give rise to characteristic $\Delta\delta_{^{13}C\alpha}$ and $\Delta\delta_{^{13}C\beta}$ profiles, these should provide a means to identify their presence in peptides. As a test, we analysed the $\Delta\delta_{^{13}C\alpha}$ and $\Delta\delta_{^{13}C\beta}$ profiles of 13 peptides that adopt β-hairpin structures in aqueous solution (Table 1). No ^{13}C data are available for the β-hairpin forming peptides reported by other groups. The N- and C-terminal residues were excluded because they can be affected by charge effects. Figure 4 shows the $\Delta\delta_{^{13}C\alpha}$ and $\Delta\delta_{^{13}C\beta}$ profiles for two of these β-hairpin forming peptides as well as their $\Delta\delta_{C\alpha H}$ profiles. The profiles corresponding to the other analysed peptides are available as Supplementary material (Figures SF1–SF6). In general, the $\Delta\delta_{^{13}C\alpha}$ profiles are in agreement with the pattern expected for the type of β-hairpin adopted by the peptide as determined by the set of NOEs. We consider that the experimental $\Delta\delta$ value of a residue is anomalous or an exception if its sign is opposite to the expected one. The peptides that adopt a high β-hairpin population show very few anomalous values at the $\Delta\delta_{^{13}C\alpha}$, $\Delta\delta_{^{13}C\beta}$ and $\Delta\delta_{C\alpha H}$ profiles, while those forming a very low β-hairpin population display a significantly larger number of exceptions (Figure 5). The number of exceptions is, in general, lower for the $\Delta\delta_{^{13}C\alpha}$ profiles than for the $\Delta\delta_{^{13}C\beta}$ and $\Delta\delta_{C\alpha H}$ profiles. In the case of the $\Delta\delta_{C\alpha H}$ values, the anomalous values usually correspond to residues that are adjacent to or facing aromatic residues and consequently affected by ring current effects.

Quantification of β-hairpin populations in peptides from $\Delta\delta_{^{13}C\alpha}$ and $\Delta\delta_{^{13}C\beta}$: Comparison with estimates from NOE intensities and from $\Delta\delta_{^{13}C\alpha H}$

The use of $\Delta\delta_{^{13}C\alpha}$ values to evaluate β-hairpin populations has been previously described (de Alba et al., 1999a; Santiveri et al., 2000). The observed chemical shifts are linearly population-weighted averages over all the states present in a fast equilibrium. However, the method assumes a simplifying two-state model for the folded–unfolded equilibrium as commonly done in all the quantification methods based on NMR parameters (Gellman, 1998; Lacroix et al., 1999; Santiveri et al., 2000). The β-hairpin population is estimated from the $\Delta\delta_{^{13}C\alpha}$ values averaged for the strand residues in the considered peptide, excluding the non-protected N- and C-terminal residues. As reference for the folded state, 100% β-hairpin, we may take the averaged $\Delta\delta_{^{13}C\alpha}$ value found in protein sheets (-1.5 ppm; Spera and Bax, 1991) or that found for the strands of the protein β-hairpins analysed here (-1.6 ppm; see above). Similarly, the $\Delta\delta_{^{13}C\beta}$ values averaged for the strand residues in the considered peptide could also be used to estimate β-hairpin populations, and two values are also available as the $\Delta\delta_{^{13}C\beta}$ reference for the 100% β-hairpin, 2.2 ppm (Spera and

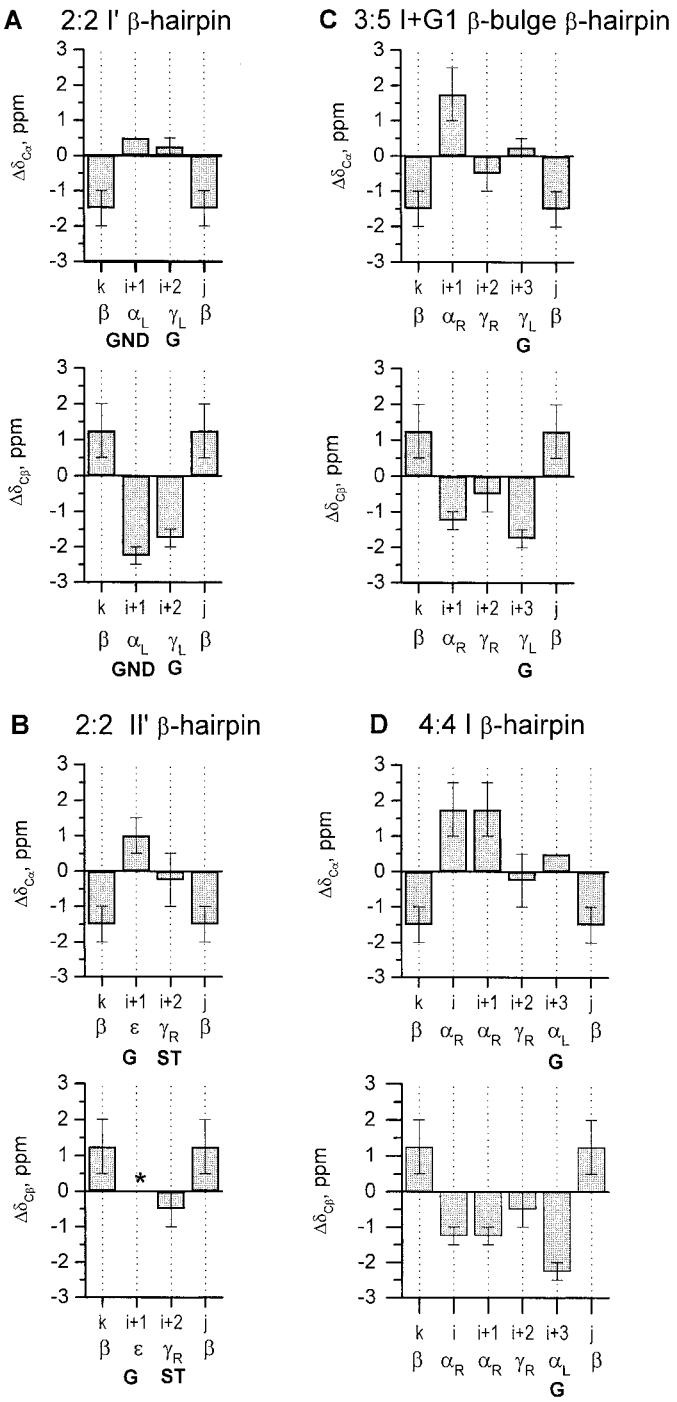

Figure 3. Expected $\Delta\delta_{13C}\alpha$ and $\Delta\delta_{13C\beta}$ values at the turn residues according to the type of β-hairpin, as classified by Sibanda et al. (1989). (A) 2:2 β-hairpins with a type I′ β-turn, (B) 2:2 β-hairpins with a type II′ β-turn, (C) 3:5 β-hairpins with a type I + G1 β-bulge turn, and (D) 4:4 β-hairpins with a type I β-turn. Values for residues adjacent to the turn are also indicated. Residues are named according to the nomenclature in Figure 1. The expected $\Delta\delta_{13C\alpha}$ and $\Delta\delta_{13C\beta}$ ranges, indicated by error bars, were obtained by analysis of $\Delta\delta_{13C\alpha}$ and $\Delta\delta_{13C\beta}$ shielding surface maps (Iwadate et al., 1999) for the characteristic ϕ,ψ angles of each residue according to their location in the regions of the Ramachandran map (as defined by Efimov, 1986) in the different β-hairpin positions (Sibanda et al., 1989). The residue or residues most frequently found at some positions are indicated in bold at the bottom. An asterisk (*) indicates a non-determined value.

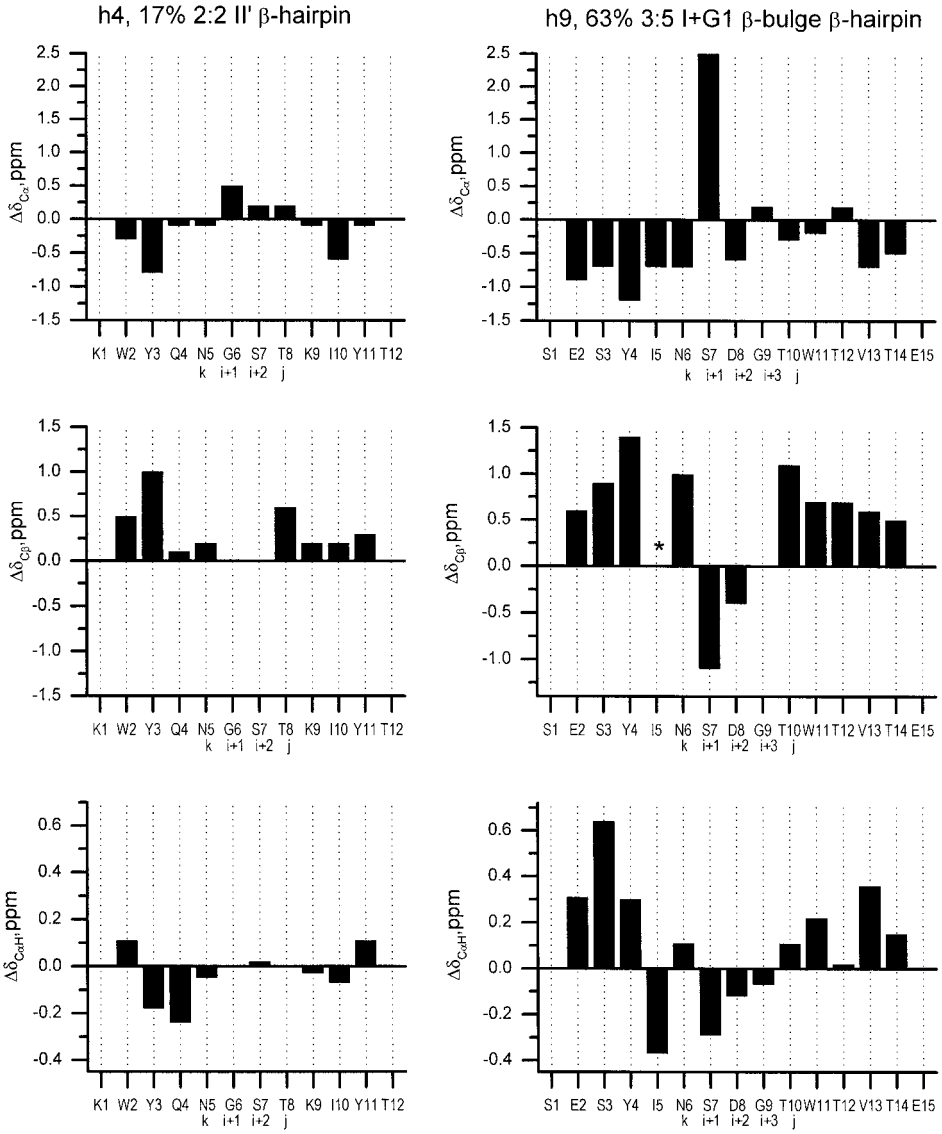

Figure 4. $^{13}C_\alpha$ (top), $^{13}C_\beta$ (middle) and $C_\alpha H$ (bottom) conformational shifts ($\Delta\delta = \delta_{(obs)} - \delta_{(random\ coil)}$ (ppm) where $\delta_{^{13}C\alpha(random\ coil)}$ and $\delta_{^{13}C\beta(random\ coil)}$ were taken from Wishart et al. (1995a)) after correction for referencing to TSP (Wishart et al., 1995b) and $\delta_{C\alpha H(random\ coil)}$ from Bundi and Wüthrich (1979) as a function of sequence for peptides h4 and h9 (Table 1). An asterisk indicates a non-determined value. For Gly, the $\Delta\delta_{C\alpha H}$ corresponds to the average value of the two $C_\alpha H$ protons. Turn residues are named according to the nomenclature in Figure 1. The β-hairpin percentages correspond to the populations evaluated from the NOE-based method.

Bax, 1991) and 1.7 ppm (this paper). We have applied these two quantification methods to 13 β-hairpin forming peptides by using the different available references for the folded state (Table 1). As a comparison, the populations for these peptides were also estimated from the intensity of the characteristic $C_\alpha H_k$-$C_\alpha H_j$ NOEs, where k and j are facing residues in a non-hydrogen-bonded site (Figure 1), and from the $\Delta\delta_{C\alpha H}$ averaged for the strand residues (Gibbs et al., 1998; Santiveri et al., 2000). The NOE-based method is the most commonly used in β-hairpins (Searle et al., 1995; de Alba et al., 1996, 1997a, b; Ramírez-Alvarado et al., 1996; Maynard et al., 1998), in spite of the estimates being only approximate. In the unfolded state the k and j $C_\alpha H$ protons are far apart, so that their NOE intensity is zero, whereas in the folded state, the β-hairpin, the NOE intensity is considered to be equal to the averaged $C_\alpha H$-$C_\alpha H$ distance observed in

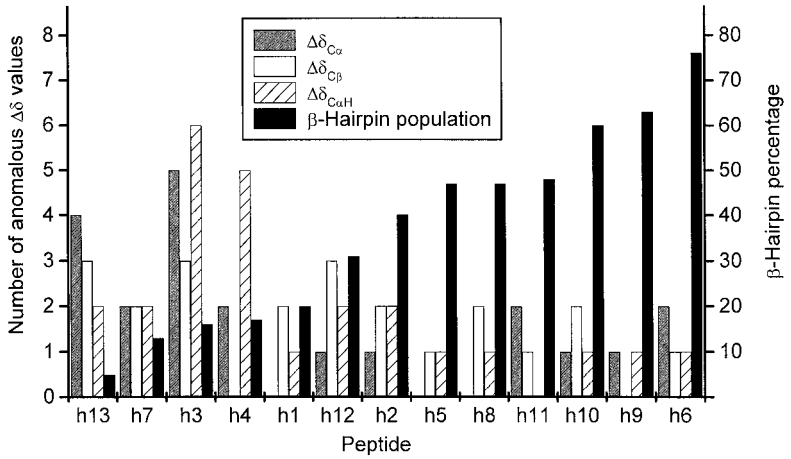

Figure 5. Histogram showing the number of anomalous values (sign opposite to the expected one or zero; left y-axis) found in the $\Delta\delta_{C\alpha}$ (grey), $\Delta\delta_{C\beta}$ (white) and $\Delta\delta_{C\alpha H}$ (striped) profiles of 13 β-hairpin forming peptides (Table 1) and the β-hairpin populations (black; right y-axis) estimated on the basis of $C_\alpha H$-$C_\alpha H$ NOE intensities (see text). The peptides are ordered by increasing β-hairpin populations from the right to the left.

antiparallel strands in proteins. Apart from the experimental error, the NOE-based estimates can be affected by small differences in the actual $C_\alpha H_j$-$C_\alpha H_k$ distance relative to the reference value and by the potential existence of different correlation times along the peptide chain and/or between the folded and the unfolded states (Gellman, 1998; Lacroix et al., 1999; Santiveri et al., 2000). The $\Delta\delta_{C\alpha H}$-based method assumes a β-hairpin–unfolded equilibrium and takes the averaged $\Delta\delta_{C\alpha H}$ value found in protein sheets (0.40 ppm; Wishart et al., 1991) as that of 100% β-hairpin.

Table 1 gives the β-hairpin percentages that were estimated by the four methods for the 13 peptides. Since some peptides have strand residues with anomalous $\Delta\delta_{C\alpha H}$, $\Delta\delta_{^{13}C\alpha}$ and $\Delta\delta_{^{13}C\beta}$ values (Figure 5), we have calculated the populations by taking into account all the strand residues except the N- and C-terminal ones, and by excluding the exceptions (Table 1). We then analysed the correlation between the β-hairpin populations obtained from each of the four quantification methods, NOE intensity, $\Delta\delta_{C\alpha H}$, $\Delta\delta_{^{13}C\alpha}$ and $\Delta\delta_{^{13}C\beta}$ (Table 2, Supplementary Table SM2 and Figure 6). The effect of using different references for the random coil δ-values was not investigated here, because it was previously found to be quite small in the case of ^{1}H δ-values (Lee and Cao, 1996; Santiveri et al., 2000). In addition, the differences between the reported random coil ^{13}C δ-values in aqueous solution (Spera and Bax, 1991; Wishart et al., 1995a) and those in 8M urea (Schwarzinger et al., 2000) are very small.

Discussion

To investigate the potential of $^{13}C_\alpha$ and $^{13}C_\beta$ chemical shifts as a means to identify the presence of β-hairpin structures in peptides, the $^{13}C_\alpha$ and $^{13}C_\beta$ conformational shifts observed in the most abundant protein β-hairpins (Figure 2) were compared to the expected values (Figure 3). The averaged $\Delta\delta_{^{13}C\alpha}$ and $\Delta\delta_{^{13}C\beta}$ values, −1.6 and +1.7 ppm, respectively, for β-strand residues in the analysed β-hairpins (Supplementary Table SM1) are in agreement with those previously reported for β-sheet regions in proteins (−1.5 and +2.2 ppm; Spera and Bax, 1991), although the averaged $\Delta\delta_{^{13}C\beta}$ value is smaller in our analysis. Regarding the loop region, the profiles found for the four kinds of β-hairpin investigated are coincident with the expected ones (see the averaged experimental profiles in Figure 2 and the expected conformational shifts in Figure 3). Apart from some slight differences in magnitude, the main discrepancy is that observed for the $\Delta\delta_{^{13}C\beta}$ value of residue j in 3:5 β-hairpins which is almost null when, being located in the β region of the Ramachandran map (Sibanda et al., 1989), it was expected to be positive and large. A plausible explanation comes from the fact that the average φ angle (−89 ± 14°) for the j residues in the analysed 3:5 β-hairpins deviates from that characteristic of the β region (−116 ± 31° in the strands of all protein β-hairpins studied here). In the $\Delta\delta_{^{13}C\beta}$ shielding surface map (Spera and Bax, 1991; Iwadate et al., 1999), the average φ angle found for j residues in 3:5 β-hairpins corresponds to a $\Delta\delta_{^{13}C\beta}$ value smaller than 1, which is closer to the ex-

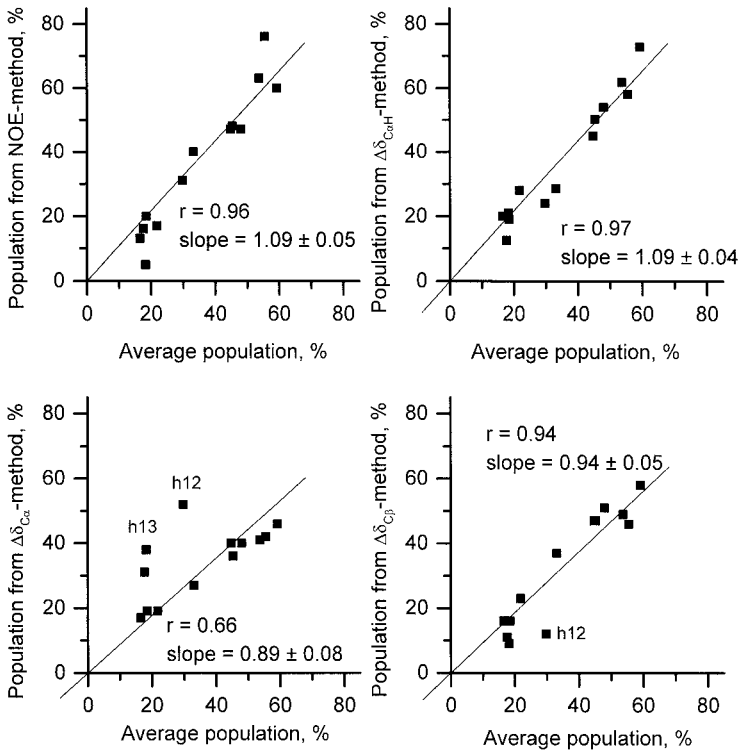

Figure 6. Correlation between the β-hairpin population formed by the peptides listed in Table 1 as estimated from different NMR parameters, NOE intensity, $\Delta\delta_{C\alpha H}$, $\Delta\delta_{C\alpha}$ and $\Delta\delta_{C\beta}$, as described in the text, and the populations averaged for the four methods. As reference for 100% β-hairpin, the averaged $\Delta\delta_{C\alpha}$ and $\Delta\delta_{C\beta}$ values for strand residues in protein β-hairpins obtained here are used. The $\Delta\delta_{C\alpha}$, $\Delta\delta_{C\beta}$ and $\Delta\delta_{C\alpha H}$ with sign opposite to that corresponding to a strand residue are not included in the estimation of β-hairpin population. The peptides showing large deviations from the fitting line are labelled.

perimental result (Figure 2C). Our analysis shows that the most abundant β-hairpins in proteins, 2:2, 3:5 and 4:4, have characteristic patterns of the $^{13}C_\alpha$ and $^{13}C_\beta$ conformational shifts. Therefore, these patterns can be of great value for identifying these structural motifs in conformational studies of peptides and proteins.

We propose herein a few criteria to identify β-hairpins on the basis of $^{13}C_\alpha$ and $^{13}C_\beta$ conformational shifts plotted as a function of the protein or peptide sequence:

(i) Two stretches of at least two consecutive residues with negative $\Delta\delta_{^{13}C\alpha}$ values and positive $\Delta\delta_{^{13}C\beta}$ values separated by 2–4 residues which include at least one presenting a positive $\Delta\delta_{^{13}C\alpha}$ value and at least one with a negative $\Delta\delta_{^{13}C\beta}$value indicate the presence of a β-hairpin. The reliability of this criterion increases with the number of residues in the two stretches.

Then, the type of β-hairpin can be determined by analysing the pattern of $^{13}C_\alpha$ and $^{13}C_\beta$ conformational shifts in the region between the two stretches as follows:

(ii) A 2:2 β-hairpin with a type I′ β-turn (Figures 2A and 3A) is characterised by two consecutive residues, i+1 and i+2, with positive $\Delta\delta_{^{13}C\alpha}$ and negative $\Delta\delta_{^{13}C\beta}$ values. The $\Delta\delta_{^{13}C\alpha}$ value of the i+2 residue (Gly in most cases; Sibanda et al., 1989; Sibanda and Thornton, 1991; Hutchinson and Thornton, 1994), is very close to zero.

(iii) The profile characteristic of the i+1 and i+2 residues of a 2:2 β-hairpin with a type II′ β-turn consists of a single residue with positive $\Delta\delta_{^{13}C\alpha}$ and negative $\Delta\delta_{^{13}C\beta}$ values, very often a Gly (Sibanda et al., 1989; Sibanda and Thornton, 1991; Hutchinson and Thornton, 1994), which is followed by a residue with $\Delta\delta_{^{13}C\alpha}$ and $\Delta\delta_{^{13}C\beta}$ values that are negative and small in absolute value (Figures 2B and 3B).

(iv) A residue, i+1, with large and positive $\Delta\delta_{^{13}C\alpha}$ value and negative $\Delta\delta_{^{13}C\beta}$ large in absolute value followed by a residue, i+2, with negative $\Delta\delta_{^{13}C\alpha}$ and $\Delta\delta_{^{13}C\beta}$ values that, in turn, is followed by a residue, i+3, showing a small and positive $\Delta\delta_{^{13}C\alpha}$ value and a negative $\Delta\delta_{^{13}C\beta}$ large in absolute value are typical

of a 3:5 β-hairpin with a I + G1 β-bulge turn (Figures 2C and 3C). The i+3 residue is a Gly in many cases (Sibanda et al., 1989; Sibanda and Thornton, 1991; Hutchinson and Thornton, 1994).
(v) A 4:4 β-hairpin with a I β-turn (Figures 2D and 3D) is characterised by two adjacent residues, i and i+1, with positive $\Delta\delta_{^{13}C\alpha}$ and negative $\Delta\delta_{^{13}C\beta}$ values followed by a residue, i+2, with negative $\Delta\delta_{^{13}C\alpha}$ and $\Delta\delta_{^{13}C\beta}$ values that is followed by a residue, i+3, with a small positive $\Delta\delta_{^{13}C\alpha}$ value and a negative $\Delta\delta_{^{13}C\beta}$ value. The i+3 residue is usually a Gly (Sibanda et al., 1989; Sibanda and Thornton, 1991; Hutchinson and Thornton, 1994). Experimental data for the $\Delta\delta_{^{13}C\beta}$ values in 4:4 β-hairpins are lacking, so that the characteristic values indicated here are based exclusively on those expected from the ϕ and ψ angles characteristic of this type of β-hairpin (Sibanda et al., 1989).

It should be noted that the $\Delta\delta_{^{13}C\alpha}$ and $\Delta\delta_{^{13}C\beta}$ sign pattern is more important than the magnitude for the identification of β-hairpins from these criteria.

The general usefulness of the above criteria in structural investigation of peptides has been demonstrated in our analysis of the $\Delta\delta_{^{13}C\alpha}$ and $\Delta\delta_{^{13}C\beta}$ profiles found in 13 β-hairpin forming peptides (Table 1). As occurs in most of these peptides, criterion (i) will recognise the presence of a β-hairpin in most cases. Of course, there will be β-hairpin forming peptides showing patterns of $\Delta\delta_{^{13}C\alpha}$ and $\Delta\delta_{^{13}C\beta}$ conformational shifts that cannot be ascribed to a specific kind of β-hairpin, as occurs in some of the analysed peptides. Even in those cases, the profiles of $\Delta\delta_{^{13}C\alpha}$ and $\Delta\delta_{^{13}C\beta}$ conformational shifts can be used as additional information to delineate β-hairpins in peptides. These conformational shift profiles are very easy to obtain because the assignment of $^{13}C_\alpha$ and $^{13}C_\beta$ chemical shifts can be readily done on the basis of the ^{1}H-^{13}C cross-correlations observed in HSQC spectra once the ^{1}H chemical shifts are assigned. Moreover, the ^{13}C natural abundance suffices to get good quality HSQC spectra at the peptide concentrations used to acquire the standard ^{1}H-NMR 2D spectra.

As an example, we describe the application of the above criteria to two peptides. Peptide h4, which adopts a 2:2 β-hairpin with a II′ β-turn in aqueous solution (de Alba et al., 1999a), and peptide h9, which forms a 3:5 β-hairpin with a I + G1 β-bulge turn (Santiveri et al., 2000). Both peptides display a profile with stretches of negative $\Delta\delta_{^{13}C\alpha}$ values flanking one residue with a positive $\Delta\delta_{^{13}C\alpha}$ value (Figure 4) which indicates the presence of a β-hairpin in both peptides (criterion i). In peptide h4, the residue with a positive $\Delta\delta_{^{13}C\alpha}$ is followed by a residue with almost null $\Delta\delta_{^{13}C\alpha}$ and $\Delta\delta_{^{13}C\beta}$ values. This pattern fits with the i+1 and i+2 residues of a 2:2 β-hairpin with a II′ β-turn (see above; Figures 2B and 3B), where the i+1 residue is a Gly, as often found in this kind of hairpins. Having identified the turn residues and the type of β-hairpin, the strand register is determined. In peptide h4, residue T8 with a positive $\Delta\delta_{^{13}C\alpha}$ instead of a negative value deviates from the expected pattern. On the basis of the profile of $C_\alpha H$ proton conformational shifts, $\Delta\delta_{C\alpha H}$, it would not even be feasible to detect the presence of a β-hairpin in peptide h4. The strands should display positive $\Delta\delta_{C\alpha H}$ values and the turn negative values (Case et al., 1994; Ösapay and Case, 1994; Wishart and Sykes, 1994; Szilágyi, 1995). The $\delta_{C\alpha H}$ values are greatly affected by the ring currents of aromatic residues and peptide h4 contains three aromatic residues, W2, Y3 and Y11. It should be noted that the population of β-hairpin adopted by peptide h4 is less than 20% (as estimated from NOE data; de Alba et al., 1999a; see Table 1). In spite of this low population, the $\Delta\delta_{^{13}C\alpha}$ profile suggests the presence of a 2:2 β-hairpin with a type II′ turn.

Concerning peptide h9 (Figure 4), the residue with a large positive $\Delta\delta_{^{13}C\alpha}$ value and a negative $\Delta\delta_{^{13}C\beta}$ large in absolute value, S7, is followed by a residue with negative $\Delta\delta_{^{13}C\alpha}$ and $\Delta\delta_{^{13}C\beta}$ values and a Gly with a small positive $\Delta\delta_{^{13}C\alpha}$ value. This is the pattern characteristic of residues i+1, i+2 and i+3 of a 3:5 β-hairpin with a type I + G1 β-bulge turn (see above; Figures 2C and 3C). The i+3 residue is a Gly, which is frequent in this type of β-hairpins. As in peptide h4, once the type of β-hairpin and the turn residues are identified, the strand register is determined. The small positive $\Delta\delta_{^{13}C\alpha}$ value observed for T12 in the strand is the only value deviating from the expected ones. The profile of $\Delta\delta_{C\alpha H}$ conformational shifts in peptide h9 is also that expected for a β-hairpin, except for the I5 and T12 strand residues that face and are adjacent to aromatic residues in the β-hairpin (Table 1).

Apart from identifying the structural motif adopted by a peptide, an accurate method to quantify the structured population is essential to evaluate the contributions of different factors to the formation and stability of structural motifs by using model peptides. In the case of β-hairpin motifs, there is no well-established method to quantify the populations adopted by peptides (Blanco et al., 1998; Gellman, 1998; Lacroix et al., 1999; Ramírez-Alvarado et al., 1999; Zerella et al., 1999; Santiveri et al., 2000). Therefore, we have investigated the use of the $\Delta\delta_{^{13}C\alpha}$ and $\Delta\delta_{^{13}C\beta}$ values

to evaluate β-hairpin populations. The variability of the populations estimated by these two methods, as well as by the NOE- and $\Delta\delta_{C\alpha H}$-based methods, for 13 β-hairpin forming peptides (Table 1) and the analysis of the pair correlation between the four methods and with the averaged populations (Table 2) indicate that: (i) exclusion of the anomalous values (those with sign opposite to the expected one or with null value) in the strands in the Δδ-based methods decreases the variations in the populations estimated by the four methods for each peptide (Tables 1 and 2). (ii) In the case of the $\Delta\delta_{^{13}C\alpha}$- and $\Delta\delta_{^{13}C\beta}$-based methods, the use of our reference values for the folded state instead of those from Spera and Bax (1991) leads to smaller variations among the populations estimated by the four methods (Table 1) and to an improvement of the pair correlations. The latter is indicated by the slopes being closer to 1 (Table 2 and Figure 6), since the slope of the correlation between the populations obtained from any two methods should be 1. (iii) The $\Delta\delta_{^{13}C\alpha}$-based populations give poor correlations (low r-values; Table 2), despite the few anomalous values displayed by the $\Delta\delta_{^{13}C\alpha}$ profiles. If peptides h12 and h13 (Figure 6) are excluded from the correlation, the r-value increases up to 0.92 (slope 0.82±0.04). The variability among the β-hairpin populations estimated by the four methods is larger for these two peptides (average standard deviation ±12 to ±20) than for all the other peptides (average standard deviation ±2 to ±13, except for peptide h6; see Table 1). This result can account for the anomalous behaviour of peptides h12 and h13. The broad range of estimated β-hairpin populations in the case of peptide h13, the peptide adopting the lowest β-hairpin population, can be due to the fact that relative experimental errors are larger for low percentages. (iv) The $\Delta\delta_{C\alpha H}$-based populations correlate very well with those from all the other parameters (r-values close to 1; Table 2), even though all the peptides, except for one, h11, show anomalous $\Delta\delta_{C\alpha H}$ values (Figure 5). (v) The NOE-based method slightly over-estimates the populations (Tables 1 and 2 and Figure 6).

On the basis of these results, we recommend the exclusion of the anomalous values in the Δδ-based estimations of β-hairpin populations and the use of the averaged $\Delta\delta_{^{13}C\alpha}$ and $\Delta\delta_{^{13}C\beta}$ values reported here as reference for the 100% β-hairpin. Nonetheless, data on more peptides are necessary to confirm and clarify the trends found here in the estimation of β-hairpin populations by different NMR parameters. We encourage authors in the field to measure and report ^{13}C chemical shifts. We think that, at present, it is advisable to evaluate the β-hairpin populations formed by peptides by all the available methods, as suggested previously (Blanco et al., 1998; Lacroix et al., 1999). The average among the estimates from all methods provides a good estimate of the β-hairpin population if the range of values resulting from the different methods is not large.

Conclusions

Protein β-hairpins have characteristic patterns of $^{13}C_\alpha$ and $^{13}C_\beta$ conformational shifts, as could be expected from their relationship to ϕ and ψ angles. From these patterns, we have derived some criteria to detect and delineate β-hairpin structures in peptides (see above) on the basis of the experimental $\Delta\delta_{^{13}C\alpha}$ and $\Delta\delta_{^{13}C\beta}$ profiles. Their application to a series of β-hairpin forming peptides demonstrates their usefulness. Regarding quantification of β-hairpin populations in peptides, the values obtained on the basis of four different NMR parameters, $C_\alpha H$-$C_\alpha H$ NOE intensities, $\Delta\delta_{^{13}C\alpha}$, $\Delta\delta_{^{13}C\beta}$ and $\Delta\delta_{C\alpha H}$, for a particular peptide display a relatively large variation. Therefore, given the absence of theoretical or experimental solid arguments in favour of any of them, we recommend the joint use of all available quantification methods.

Supplementary material available

A table (Table SM1) listing the analysed protein β-hairpins. A table (Table SM2) giving the r-values and the slopes for all the pair correlations between β-hairpin populations formed by the peptides listed in Table 1. Tables listing the ^{1}H and ^{13}C δ values of peptides h1, h2, h5, h6, h7, h8, h10, h11, h12, and h13 (Tables SM3–SM12). Six figures (Figures SF1–SF6) showing the $\Delta\delta_{^{13}C\alpha}$, $\Delta\delta_{^{13}C\beta}$ and $\Delta\delta_{C\alpha H}$ profiles for peptides h1, h2, h3, h5, h6, h7, h8, h10, h11, h12 and h13.

Acknowledgements

We thank Mrs. C. López, Mr. A. Gómez and Mr. L. de la Vega for their technical assistance. We are grateful to Drs. D.V. Laurents, F.J. Blanco and J. Santoro for their critical reading of the manuscript and to Dr. L. Szilágyi for helpful discussions. This work was supported by the Spanish DGYCT project no. PB98-0677

and European project no. CEE B104-97-2086. C.M.S. is a recipient of a pre-doctoral fellowship from the Autonomous Community of Madrid, Spain.

References

Aue, W.P., Bertholdi, E. and Ernst, R.R. (1976) *J. Chem. Phys.*, **64**, 2229–2246.

Bax, A. and Subramanian, J. (1986) *J. Magn. Reson.*, **65**, 355–360.

Beger, R.D. and Bolton, P.H. (1997) *J. Biomol. NMR*, **10**, 129–142.

Blanco, F.J., Ramírez-Alvarado, M. and Serrano, L. (1998) *Curr. Opin. Struct. Biol.*, **8**, 107–111.

Bodenhausen, G. and Ruben, D.J. (1980) *Chem. Phys. Lett.*, **69**, 185–189.

Bothner-By, A.A., Stephens, R.L., Lee, J.M., Warren, C.D. and Jeanloz, R.W. (1984) *J. Am. Chem. Soc.*, **106**, 811–813.

Braunschweiler, L. and Ernst, R.R. (1983) *J. Magn. Reson.*, **53**, 521–528.

Buckley, P., Edison, A.S., Kemple, M.D. and Prendergast, F.G. (1993) *J. Biomol. NMR*, **3**, 639–652.

Bundi, A. and Wüthrich, K. (1979) *Biopolymers*, **18**, 285–297.

Case, D.A., Dyson, H.J. and Wright, P.E. (1994) *Methods Enzymol.*, **239**, 392–416.

Cornilescu, G., Delaglio, F. and Bax, A. (1999) *J. Biomol. NMR*, **13**, 289–302.

Daura, X., Antes, I., van Gunsteren, W.F., Thiel, W. and Mark, A.E. (1999) *Proteins*, **36**, 542–555.

de Alba, E. (1997) *NMR Study of the Formation of β-Sheet Motifs in Peptides*, Ph.D. Thesis, Facultad de Ciencias Químicas, Universidad Complutense de Madrid, Spain.

de Alba, E., Jiménez, M.A., Rico, M. and Nieto, J.L. (1996) *Folding Des.*, **1**, 133–144.

de Alba, E., Rico, M. and Jiménez, M.A. (1997a) *Protein Sci.*, **6**, 2548–2560.

de Alba, E., Jiménez, M.A. and Rico, M. (1997b) *J. Am. Chem. Soc.*, **119**, 175–183.

de Alba, E., Rico, M. and Jiménez, M.A. (1999a) *Protein Sci.*, **8**, 854–865.

de Alba, E., Rico, M. and Jiménez, M.A. (1999b) *Protein Sci.*, **8**, 2234–2244.

de Dios, A.C., Pearson, J.G. and Oldfield, E. (1993) *Science*, **260**, 1491–1496.

Dyson, H.J. and Wright, P.E. (1991) *Annu. Rev. Biophys. Biophys. Chem.*, **20**, 519–538.

Efimov, A.V. (1986) *Mol. Biol. (Mosk)*, **20**, 250–260.

Gellman, S.H. (1998) *Curr. Opin. Chem. Biol.*, **2**, 717–725.

Gibbs, A.C., Kondejewski, L.H., Gronwald, W., Nip, A.M., Hodges, R.S., Sykes, B.D. and Wishart, D.S. (1998) *Nat. Struct. Biol.*, **5**, 284–288.

Gronenborn, A.M. and Clore, G.M. (1994) *J. Biomol. NMR*, **4**, 455–458.

Guerois, R., Cordier-Ochsenbein, F., Baleux, F., Huynh-Dinh, T., Neumann, J.-M. and Sanson, A. (1998) *Protein Sci.*, **7**, 1506–1515.

Hutchinson, E.G. and Thornton, J.M. (1994) *Protein Sci.*, **3**, 2207–2216.

Iwadate, M., Asakura, T. and Williamson, M.P. (1999) *J. Biomol. NMR*, **13**, 199–211.

Jeener, J., Meier, B.H., Bachmann, P. and Ernst, R.A. (1979) *J. Chem. Phys.*, **71**, 4546–4553.

Kumar, A., Ernst, R.R. and Wüthrich, K. (1980) *Biochem. Biophys. Res. Commun.*, **95**, 1–6.

Kuszewski, J., Qin, J., Gronenborn, A.M. and Clore, G.M. (1995) *J. Magn. Reson.*, **B106**, 92–96.

Lacroix, E., Kortemme, T., López de la Paz, M. and Serrano, L. (1999) *Curr. Opin. Struct. Biol.*, **9**, 487–493.

Laws, D.D., de Dios, A.C. and Oldfield, E. (1993) *J. Biomol. NMR*, **3**, 607–612.

Le, H., Pearson, J.G., de Dios, A.C. and Oldfield, E. (1995) *J. Am. Chem. Soc.*, **117**, 3800–3807.

Lee, M.S. and Cao, B. (1996) *Protein Eng.*, **9**, 15–25.

Lee, M.S., Palmer III, A.G. and Wright, P.E. (1992) *J. Biomol. NMR*, **2**, 307–322.

Luginbühl, P., Szyperski, T. and Wüthrich, K. (1995) *J. Magn. Reson.*, **B109**, 229–233.

Maynard, A.J., Sharman, G.J. and Searle, M.S. (1998) *J. Am. Chem. Soc.*, **120**, 1996–2007.

Oldfield, E. (1995) *J. Biomol. NMR*, **5**, 217–225.

Ösapay, K. and Case, D.A. (1994) *J. Biomol. NMR*, **4**, 215–230.

Ramírez-Alvarado, M., Blanco, F.J. and Serrano, L. (1996) *Nat. Struct. Biol.*, **3**, 604–612.

Ramírez-Alvarado, M., Kortemme, T., Blanco, F.J. and Serrano, L. (1999) *Bioorg. Med. Chem.*, **7**, 93–103.

Rance, M. (1987) *J. Magn. Reson.*, **74**, 557–564.

Redfield, A.G. and Kuntz, S.D. (1975) *J. Magn. Reson.*, **19**, 250–254.

Reily, M.D., Thanabal, V. and Omicinsky, D.C. (1992) *J. Am. Chem. Soc.*, **114**, 6251–6252.

Santiveri, C.M., Rico, M. and Jiménez, M.A. (2000) *Protein Sci.*, **9**, 2151–2160.

Schwarzinger, S., Kroon, G.J., Foss, T.R., Wright, P.E. and Dyson, H.J. (2000) *J. Biomol. NMR*, **18**, 43–48.

Searle, M.S., Williams, D.M. and Packman, L.C. (1995) *Nat. Struct. Biol.*, **2**, 999–1006.

Sibanda, B.L. and Thornton, J.M. (1985) *Nature*, **316**, 170–174.

Sibanda, B.L., Blundell, T.L. and Thornton, J.M. (1989) *J. Mol. Biol.*, **206**, 759–777.

Sibanda, B.L. and Thornton, J.M. (1991) *Methods Enzymol.*, **202**, 59–82.

Smith, C.K. and Regan, L. (1997) *Acc. Chem. Res.*, **30**, 153–161.

Spera, S. and Bax, A. (1991) *J. Am. Chem. Soc.*, **113**, 5490–5492.

Szilágyi, L. (1995) *Prog. NMR Spectrosc.*, **27**, 325–443.

Wishart, D.S., Sykes, B.D. and Richards, F.M. (1991) *J. Mol. Biol.*, **222**, 311–333.

Wishart, D.S. and Sykes, B.D. (1994) *Methods Enzymol.*, **239**, 363–392.

Wishart, D.S., Bigam, C.G., Holm, A., Hodges, R.S. and Sykes, B.D. (1995a) *J. Biomol. NMR*, **5**, 67–81.

Wishart, D.S., Bigam, C.G., Yao, J., Abildgaard, F., Dyson, H.J., Oldfield, E., Markley, J.L. and Sykes, B.D. (1995b) *J. Biomol. NMR*, **6**, 135–140.

Wright, P.E., Dyson, H.J. and Lerner, R.A. (1988) *Biochemistry*, **27**, 7167–7175.

Wüthrich, K., Billeter, M. and Braun, W. (1984) *J. Mol. Biol.*, **180**, 715–740.

Wüthrich, K. (1986) *NMR of Proteins and Nucleic Acids*, Wiley, New York, NY.

Yao, J., Dyson, J. and Wright, P.E. (1997) *FEBS Lett.*, **419**, 285–289.

Zerella, R., Ekens, P.A., Ionides, J.M., Peckman, L.C., Trotter, B.W., MacKay, J.P. and Williams, D.H. (1999) *Protein Sci.*, **8**, 1320–1331.